

Deuterium-induced volume expansion in Fe_{0.5}V_{0.5}/V superlatticesGunnar K. Pálsson,¹ Vassilios Kapaklis,¹ Joseph A. Dura,² Julie Jacob,¹ Sumedha Jayanetti,^{1,3} Adrian R. Rennie,¹ and Björgvin Hjörvarsson¹¹*Department of Physics and Astronomy, Uppsala University, P.O. Box 516, S-75120 Uppsala, Sweden*²*NIST Center for Neutron Research, National Institute of Standards and Technology, 100 Bureau Drive, Mail Stop 6102, Gaithersburg, Maryland 20899-6102, USA*³*Department of Physics, University of Colombo, Box 1490, Colombo, Sri Lanka*

(Received 22 September 2010; published 16 December 2010)

Neutron reflectometry was used to investigate the deuterium uptake in a thin metal superlattice that displays an anisotropic elastic response [Fe_{0.5}V_{0.5}/V (6/21 monolayers)]. We see evidence of the presence of a coexistence region which has never before been seen in vanadium-based superlattices. The loading process is completely reversible from which we conclude that the phases must be coherent, in stark contrast to bulk VD_x, where the two-phase region displays hysteresis. The deuterium-induced volume expansion exhibits changes in slope that correlate with the plateau region and the expansion is comparable and even larger than in the bulk. The spectacular cooperation between the elastic fields seems to be found only in one-dimensionally confined structures with biaxial compressive strain states.

DOI: [10.1103/PhysRevB.82.245424](https://doi.org/10.1103/PhysRevB.82.245424)

PACS number(s): 61.05.fj, 68.55.Ln, 61.05.cm, 61.05.cp

I. INTRODUCTION

The changes in the physical properties of metal hydrides confined to low-dimensional geometries constitute an exciting research avenue into nanophysics. For example, hydrogen can be used to continuously and reversibly tune the magnetic interlayer exchange coupling in Fe/V (001) superlattices¹ and highly textured Fe/Nb multilayers,² as well as strongly enhance the magnetoresistance of embedded Gd₃CoH_x nanowires in Gd (Ref. 3). There is also a considerable interest of trying to alter the thermodynamic properties of metal-hydride particles by reducing their size into the nanoregime.⁴⁻⁹ This is due, in part, to the high surface-to-volume ratio where surface states have elevated importance. Nanosized and nanoporous materials are expected to exhibit faster kinetics of uptake for the same reason.

When hydrogen is confined to extremely thin layers, the thermodynamic properties are strongly affected by the finite size, as well as by the strain state of the hydrogen absorbing layers.¹⁰ For example, the hydrogen-hydrogen interaction in vanadium switches from being repulsive to attractive when changing the elastic boundary conditions by sandwiching vanadium between Mo or Fe.¹¹⁻¹⁵ Nevertheless, the influence of size, strain, and confinement on the phase diagram is not fully understood. A better understanding of these phenomena is desirable since these underpin the mechanisms through which the physical properties of the materials are modified.

The volume changes are often described by hydrogen-induced expansion coefficients, k , within a phase of continuous solubility. Tabulated values of k for bulk materials are found in most comprehensive hydrogen reference books and are defined by

$$\frac{\Delta V}{V} = kx = \frac{\Delta v}{\Omega}x, \quad (1)$$

where V is the volume of the sample, x is the concentration in atomic ratio, Ω is the volume per metal atom, and Δv is the volume change per hydrogen atom.

The expansion coefficients found for the transition-metal hydrides are remarkably similar, suggesting that the effective volume of a dissolved hydrogen atom is close to constant ($k = \Delta v / \Omega \approx 0.18$).¹⁶ The expansion coefficients of thin films and superlattices are less explored and cannot be assumed to be the same as in bulk. The early work on the hydrogen induced volume changes in vanadium-based superlattices yielded surprising results: the expansion coefficient of the vanadium layers was determined to be $k_{\text{Mo/V}} = 0.04$,¹⁷ which is exceedingly small compared to the bulk value $k_b = 0.19$. These experiments were performed using Mo/V (001) (2 nm/2 nm) (001) superlattices, in which the vanadium is under biaxial tensile strain. The notation A/B N/M will refer to a superlattice comprised of material A and B with N and M thicknesses, respectively.

Andersson *et al.*¹⁸ measured an unusually large expansion coefficient ($k_{\text{Fe/V}} = 0.35$) in Fe/V (001) (1.8 nm/1.6 nm) superlattices at concentrations below 0.1 in H/V (atomic ratio). The authors concluded that this result could not be explained by clamping effects. Nonetheless, the strong biaxial compressive strain state of the vanadium layers was inferred to align the axis of all the local strain fields in the [001] direction, causing an exclusive octahedral z -site (O_z) occupancy. A complete alignment of the axes of the strain fields is expected to result in an additional expansion, if the expansion is restricted to one dimension by adhesion to a substrate. This result remains unexplained however. The phase diagram of Fe/V (1.8 nm/1.6 nm) is strongly altered from bulk VH_x where no coexistence region ($\alpha + \beta$) is found above room temperature and the disordered α phase has the same configuration as the β_2 phase of VH_x.

The above results were obtained using x-ray diffraction, which was recently demonstrated to be unsuitable for accurate determination of the volume change for reversible absorption in superlattices¹⁹ as well as for irreversible processes in multilayers.²⁰ The main reason is that x-ray diffraction does not capture the volume change originating from the disordered part of the structure, providing the possibility for a new interpretation of diffraction data, presented

in earlier works. The determination of the hydrogen concentration also constitutes a significant uncertainty in the determined expansion coefficients.

The volume change and the concentration can be measured simultaneously and independently using neutron reflectivity. This approach has previously been used to determine the deuterium and hydrogen concentration in Mo/V superlattices, revealing the size of depleted regions at the interfaces.²¹ *In situ* determination of the volume expansion coefficient was made in Mo_{0.5}V_{0.5}/V superlattices, using the same technique.¹³ The subscripts denote the atomic fraction of V in Mo in the alloy. The volume change and the concentration are measured through shifts in the superlattice peaks and changes in the integrated intensity respectively.

In the present study we examine how volume changes scale with concentration in a finite-size system which consists of a weakly strained Fe_{0.5}V_{0.5}/V 6/21 monolayer (ML) superlattice. We present results using *in situ* neutron reflectivity which allows highly accurate and unambiguous determination of the expansion coefficients in a wide concentration range and at two different temperatures.

II. EXPERIMENTAL DETAILS

A. Sample design

The amplitude of a scattered neutron wave from a nucleus is governed by its bound coherent neutron-scattering length, b , which are tabulated.²² The scattering length density of a material is defined by

$$\rho = \sum_i n_i b_i, \quad (2)$$

where i is the i th of m atoms and n_i is the number density. The composition of the FeV alloy was chosen to match the scattering length density of VD_{0.7} which corresponds to the maximum expected concentration at the highest pressure available to us. This enhances the resolution of the concentration determination. Vanadium has a small negative neutron-scattering length ($b_V = -0.382$ fm) while an alloy of Fe_{0.5}V_{0.5} ($b_{Fe} = +9.45$ fm for pure Fe) has a positive value. This sample design results in a good contrast ($\Delta\rho = \rho_{FeV} - \rho_V$) for neutrons in the vanadium layers, as shown in panel (a) of Fig. 1. The presence of deuterium in the vanadium layers results in an increased scattering length density of the vanadium layers ($b_D = +6.671$ fm) and thereby decreasing contrast, as shown in panel (b) of Fig. 1. The scattering length density of VD _{x} can be written as

$$\rho_{VD(x)} = n_V b_V + n_D b_D = \Gamma_V d_V b_V + \Gamma_V \frac{\Gamma_D}{\Gamma_V} d_D b_D, \quad (3)$$

where Γ_i is the area density of atoms of element i and d_i is the partial thickness of element i . We assume that the area density of vanadium does not change during the absorption which allows us to define $x = \Gamma_D / \Gamma_V$ as a concentration ratio of deuterium atoms to vanadium atoms. The contrast can also be tuned to zero, as illustrated in panel (c) of Fig. 1.

Within the kinematic approximation, the neutron reflectivity is the square of the Fourier transform of the scattering

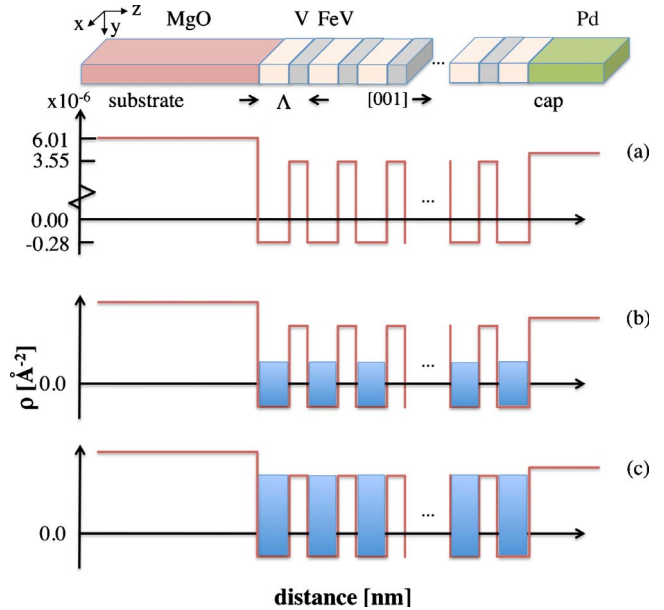


FIG. 1. (Color online) Schematic view of a superlattice and the scattering length density profile of an ideal superlattice, panel (a). The chemical repetition distance is denoted as Λ . When deuterium is absorbed into vanadium, the scattering length density changes, shown in blue. Panel (b) symbolizes a concentration of 0.35 D/V (atomic ratio), and complete matching is around 0.7 in D/V, as shown in panel (c).

length density profile shown in Fig. 1 and can be thought of as composed of a sum of an infinite number of Fourier components. The first component is a sine wave that has its maximum value in the center of one of the layers. The amplitude of the wave is proportional to the contrast which can be modified by deuterium. The change in amplitude of the first Fourier component thus represents a change in deuterium concentration and a change in its period yields the change in thickness in the growth direction. The above argument is not restricted to square wave modulations but holds as long as the modulation is symmetric. Below we will give a detailed account of the calculation of the deuterium concentration from the contrast.

B. Sample preparation and structural characterization

The Fe_{0.5}V_{0.5}/V (6/21) ML superlattice with 100 repetitions was grown on a 20 × 20 × 0.5 mm³ polished single-crystal MgO (001) substrate using UHV-based magnetron cosputtering.²³ The base pressure in the system was 2×10^{-7} Pa prior to deposition with the dominating residual gas being hydrogen. The sample was deposited from targets of iron and vanadium onto the substrate held at 573 K. Argon, with purity better than 99.9999% at a pressure of 0.27 Pa was used as the sputtering gas. The deposition rates of Fe and V were 0.0134 nm s⁻¹ and 0.0143 nm s⁻¹, respectively. The first vanadium layer was directly deposited onto the MgO substrate and the superlattice was capped with a vanadium layer followed by a 10 nm palladium layer. The palladium was sputtered from a target with 99.99% purity after cooling the sample to room temperature. The palladium layer

acts as a catalyst for the deuterium dissociation and protects the underlying structure from oxidation.

Transmission electron microscopy (TEM) measurements were made in the Uppsala Microstructure Laboratory using a JEOL 2000 FX11 transmission electron microscope. Bright-field images were taken at a magnification of $80\,000\times$ at a voltage of 200 kV and a beam current of $100\ \mu\text{A}$.

X-ray reflectivity and diffraction were measured using a Bruker Discovery D8. The operating wavelength of the instrument is $\lambda=0.15406\ \text{nm}$ (Cu $K\alpha_1$ radiation) which is selected by a Göbel mirror and a beam compressor yielding a wavelength spread of $\Delta\lambda/\lambda=1\times 10^{-4}$. X-ray and neutron reflectivity curves were fitted using GENX (Ref. 24) which uses the Parratt²⁵ formalism and takes dynamic effects such as multiple reflections, absorption and refraction into account. The program also includes instrumental resolution and geometric corrections.

C. Neutron reflectivity and loading procedure

Neutron reflectivity measurements were performed at the NG1 reflectometer at NIST, Gaithersburg. A similar instrument has been described in the literature.²⁶ The neutron wavelength was $0.475(5)\ \text{nm}$ and a post sample analyzer was used to optimize signal to noise. The slits were changed continuously as specular intensity was recorded to provide a constant $\Delta Q/Q$ and footprint, where Q is the length of the scattering vector \mathbf{Q} , and is given by

$$Q = \frac{4\pi}{\lambda} \sin \theta, \quad (4)$$

with λ being the wavelength and θ is half the scattering angle. The sample was mounted inside a vacuum chamber which can be filled with deuterium of 99.9% of isotopic purity. The gas pressure inside the chamber was monitored using Baratron membrane gauges suitable for different ranges from 133.3 Pa to 0.133 MPa. The sample temperature was kept constant within 50 mK with the help of a Lakeshore temperature controller. The temperature sensor was later found not to be in good thermal contact. A more accurate temperature was measured after the experiments had finished. We still assign a large error bar to the absolute value of the temperature, $\pm 5\ \text{K}$.

The deuterium pressure was increased in steps and sufficient time was given for the sample to reach equilibrium. The uptake was continuously monitored by the changes in the position and the intensity of the first Bragg peak. The deuterium concentration was determined from the area of a Gaussian function fitted to the first-order peak, after an appropriate background correction. As more deuterium enters the vanadium layers, the difference in the scattering length densities between the vanadium and $\text{Fe}_{0.5}\text{V}_{0.5}$ layers decreases, resulting in a decreased intensity of the first order Bragg peak. The sample was realigned after each pressure step to ensure well-defined scattering conditions. Rocking curves across the first Bragg peak were recorded regularly to verify that no in-plane broadening of the peak occurred that could be misinterpreted as a concentration change.

D. Deuterium concentration and volume expansion

The reflectivity amplitude from a superlattice can be expressed using the kinematic approximation as

$$r(Q) = \frac{4\pi}{iQ} \int f(z) e^{iQz} dz, \quad (5)$$

where $f(z)$ is the ideal scattering length density profile shown in Fig. 1. A detailed derivation of the integral can be found in Ref. 27.

The reflectivity intensity of superlattice peak m is obtained by using the condition of constructive interference and taking the absolute square of the reflectivity amplitude,

$$R\left(Q = \frac{2\pi m}{\Lambda}\right) = \left[\frac{2N\Lambda^2}{\pi m^2} (\rho_{\text{FeV}} - \rho_{\text{V}}) \sin\left(\frac{\pi m d_{\text{V}}}{\Lambda}\right) \right]^2, \quad (6)$$

where d_{FeV} and d_{V} are the thicknesses of the layers, $\Lambda = d_{\text{FeV}} + d_{\text{V}}$ is the chemical repeat distance, and N is the number of repeats.

As can be seen from Eq. (6) the reflectivity depends on the square of the contrast as qualitatively discussed above. The observed peak intensity is therefore a direct measure of the deuterium concentration in the vanadium layers. Combining Eqs. (3) and (6) the deuterium concentration, x , obtained from the intensity ratio of the first-order superlattice peaks is

$$x = \frac{\Delta\rho(0)}{\Gamma_{\text{V}} d_{\text{V}}(x) b_{\text{D}}} \left(1 - \frac{\sqrt{R(x)} \Lambda^2(0) \sin[\pi d_{\text{V}}(0)/\Lambda]}{\sqrt{R(0)} \Lambda^2(x) \sin[\pi d_{\text{V}}(x)/\Lambda(x)]} \right). \quad (7)$$

The concentration depends thus primarily on the square roots of the reflectivity intensity ratios and the changes in thickness of the V layers. The thickness dependence was neglected in the analysis done by Leiner *et al.*¹³ It is worth noting that (i) the changes in thickness are much smaller than the changes in intensity and (ii) the thickness changes have a tendency to cancel in Eq. (7), somewhat justifying their approximation.

Fe/V(001) superlattices are known^{1,14,18} to withstand repeated cycling of hydrogen, without loss in structural coherency. Since stress relief through misfit dislocations and cracking and peeling is not observed, any in-plane expansion must be negligible. The structure was found to be unchanged by cyclic loading of deuterium as seen by x-ray reflectivity and x-ray diffraction measurements before and after the neutron experiments. Resistance measurements were performed separately on a similar sample with 25 repeats which showed no irreversible changes with deuterium loading.

Thus it is sufficient to determine the out-of-plane expansion to accurately measure the volume changes. The changes in the vanadium thickness is thus determined from the experimentally measured changes in Λ and simulated values of d_{FeV} ,

$$\frac{\Delta d_{\text{V}}}{d_{\text{V}}} = \frac{\Delta \Lambda}{\Lambda - d_{\text{FeV}}}. \quad (8)$$

The assumption that the deuterium concentration of the alloy can be neglected was validated by investigating the hydrogen uptake of a series of $\text{V}_x\text{Fe}_{1-x}$ single crystals grown on MgO

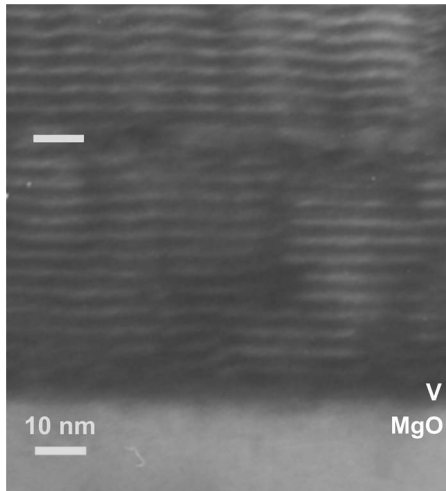


FIG. 2. Transmission electron microscope image of part of the superlattice closest to the substrate. A defect (missing layer) is located around the 13th period from the substrate as marked by the white line. The dark lines correspond to vanadium and the lighter to FeV.

(001). The composition of the FeV alloy was varied between 0.1 and 0.5 and the hydrogen uptake was determined by measuring the changes in resistance with pressure at various temperatures. For low concentrations the solubility is governed by the enthalpy of solution with an exponential dependence (Sievert's law). The enthalpy of $V_{0.5}Fe_{0.5}$ alloy was measured and found to be higher than in Pd which is $H_s^0 = +0.10$ eV/H atom compared to $H_s^0 = -0.28$ eV per atom for V. Thus the deuterium concentration in the FeV alloy can safely be ignored.²⁸

III. RESULTS

A. Sample structure

One of the 100 vanadium layers was found to be missing, which was confirmed by x-ray reflectivity and neutron reflectivity data and simulations, and transmission electron microscopy. The effect of the missing layer is included in the simulations and was found to have negligible influence on the accuracy of the deduced expansion coefficients. The missing vanadium layer results in one thicker FeV layer, which influences the quality of the subsequently deposited layers. This is seen in Fig. 2 which displays a part of the sample closest to the substrate. The defect is clearly visible around 13 repeat distances from the substrate, marked by a white bar in the figure. Note that the image has been artificially brightened for clarity.

Raw data from x-ray diffraction of the as-deposited sample are shown in Fig. 3, measured with a position sensitive detector. The width (full width at half maximum) of the fundamental peak (labeled 0 in Fig. 3) is 0.094° , which corresponds to a coherence length of 109 nm, i.e., close to 26 repetitions. This suggests that roughly a quarter of the sample is scattering coherently in the [001] direction. This is much larger than the thickness of the repeat distance and justifies our use of the term superlattice when referring to the

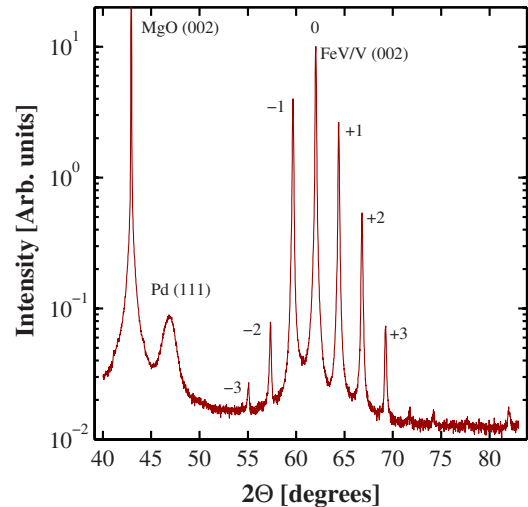


FIG. 3. (Color online) X-ray diffraction pattern of the as-deposited sample. The fundamental peak of the superlattice is indexed as zeroth order and corresponds to the average lattice parameter of the period. Satellites labeled, $\pm n$ are visible up to at least third order which is indicative of sharp interfaces between the alloy and V. Also visible in the figure are the (002) peak from MgO and a peak arising from textured Pd (111) planes.

sample. A rocking scan across the (002) Bragg peak, parallel to the plane of the film, revealed a mosaicity of 0.26° which can be compared to other Fe/V superlattices in the literature.^{19,29} The modulation in the chemical composition is good, as seen by the number of superlattice peaks which is in agreement with results from x-ray reflectivity fits which gave 4.7 ML as the root mean square roughness. The TEM image in Fig. 2 is a local probe of the sample structure but confirms a relatively good layering of the superlattice.

Figure 4 shows complete neutron reflectivity patterns at 491(3) K in vacuum and 0.132 MPa. The solid lines are fits generated by GENX. The model input to the fitting program was, as seen in Fig. 1 with the distortion shown in Fig. 2 taken into account. The fringes that appear before the first superlattice peak are due to interference between the neutron reflecting from the substrate interface and the top of the defect. The total thickness of the superlattice is several hundred nanometers and would give rise to fringes that are much narrower. These were indeed seen in the region close to the critical edge. The complete measurements were made at the indicated pressures only and the fits serve to (i) verify the initial structure, (ii) rule out the influence of the distortion on the results, (iii) act as a consistency check at one concentration for the simplified approach of using Eq. (7). A selected number of scans around the first superlattice peak as a function of pressure are shown in the inset to highlight the changes in intensity upon absorption of deuterium. As is apparent, shifts toward lower Q values come from changes in Λ and changes in intensity come from the loading of deuterium.

An interface region with reduced deuterium content was required to quantitatively reproduce the increase in the intensity of the third-order reflectivity peak at 0.132 MPa. The presence of depleted layers close to the interface are well

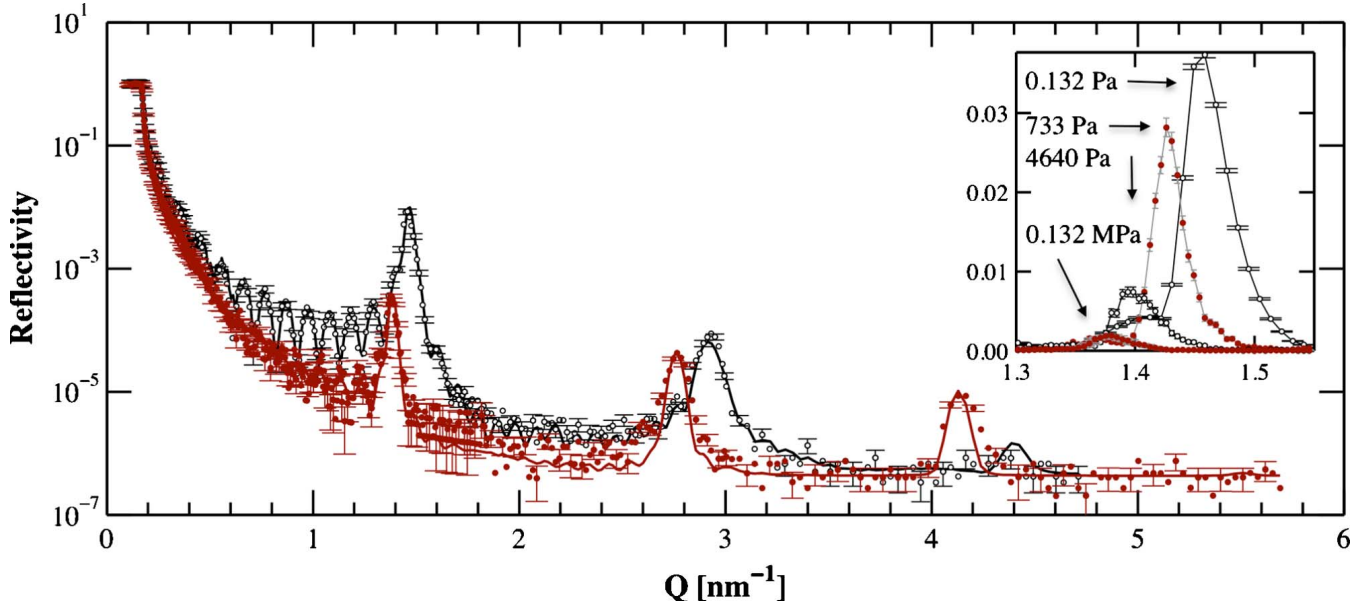


FIG. 4. (Color online) Neutron reflectivity curves for the superlattice at 0.1 Pa (open) and 0.132 MPa (filled) D₂ pressures. The solid curves are fits obtained using GenX. The inset shows four of the many scans around the first Bragg peak on a linear scale at different pressures. The pressures are (in order of decreasing intensity) 0.132 Pa, 733 Pa, 4640 Pa, and 0.132 MPa. Note the large changes in the intensity during deuterium loading. The solid lines in the inset are guides to the eye. The error bars, $\pm 1\sigma$, are only shown for every third data point for clarity.

known in Mo/V superlattices,^{21,30-32} Fe/V structures,¹⁵ and Mo_{0.5}V_{0.5}/V superlattices¹³ and the results we obtained are consistent with these findings. Thus, the average concentration across the whole V layer and the concentration in the center are not the same as discussed in Sec. II A. Using GENX, a size of $L=0.1$ nm was found at both sides of the V layers, assuming complete depletion. Unless otherwise stated we will refer to the interior concentration in the vanadium layers. To correct the volume change to reflect the interior volume change the following equation can be used:

$$\frac{\Delta d_V^{int}}{d_V^{int}} = \frac{\Delta d_V}{d_V} \left(1 + \frac{2L}{d_V} \right). \quad (9)$$

B. Elastic response

In Fig. 5 the concentration, determined from the intensity of the first superlattice peak, vs pressure, is shown. A plateau is clearly visible for each data set indicating a coexistence region of some sort. It is not a spinodal region since we are confident that the points on the plateau are taken at thermodynamic equilibrium. We infer from the relative flatness of the plateau that we are below a phase boundary which is remarkable considering that the transition in bulk VD_x is around 406 K. This is also completely contrary to what is found in symmetric superlattices of Fe/V loaded with hydrogen¹⁵ where no coexistence region has been found. Since the superlattice structure was found to be unchanged by cyclic deuterium loading as discussed in Sec. II D we conclude that the phase transition in the coexistence region must be coherent. Coherency in this context means that associated with a change in phase is a continuous change in

lattice parameter. Incoherent phases are characterized by generation of defects and hysteresis. Two regions can be identified on either side of the plateau that probably correspond to single phases/configurations.

In Fig. 6 we show the change in thickness of the vanadium layers with concentration. Significant scattering of the data points is observed at the lowest concentrations. In this region the accuracy of the concentration determination is the poorest. We observe no temperature dependence which is in line with bulk observations. It is natural to fit the data on either side of the coexistence region to separate lines since these regions are expected to correspond to different phases/

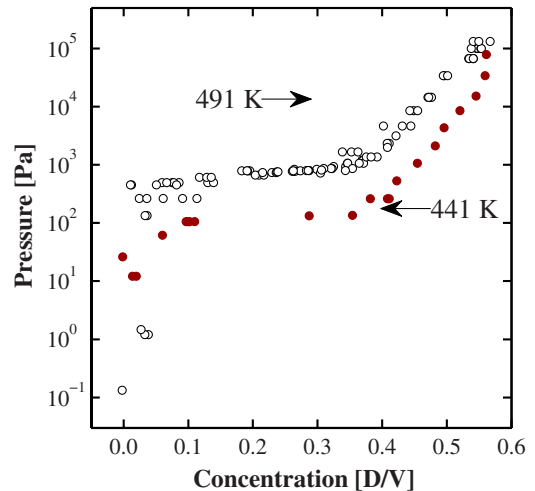


FIG. 5. (Color online) Isotherms at 491 K (black) and 441 K (red), respectively, obtained from the intensity of the first-order superlattice peak.

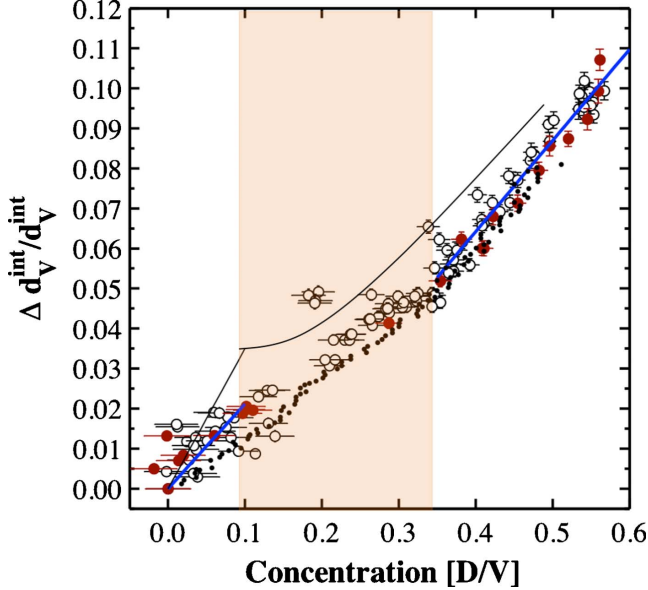


FIG. 6. (Color online) Volume expansion of the vanadium layers in a $\text{Fe}_{0.5}\text{V}_{0.5}/\text{V}$ superlattice versus deuterium concentration. The black open and red filled circles correspond to 491 K and 441 K, respectively. The points were extracted from shifts in the first-order superlattice peak and its integrated intensity. The shaded region marks the coexistence region as found from the isotherms. The solid blue lines are linear fits to the data. The thin black line is from hydrogen loaded Fe/V (1.8 nm/1.6 nm) from Ref. 18. The smaller filled circles are for MoV/V and taken from Ref. 13.

configurations. The slope in the lower region is 0.21(2) and it is 0.228(8) in the high region. We also note that the expansion in the coexistence region is clearly lower than on either side.

For comparison, we show data from a hydrogen loaded Fe/V (1.8 nm/1.6 nm) superlattice (black solid line) in a strongly compressive strain state (Ref. 18). We see that the current sample exhibits a distinctly different behavior. We also show data from a MoV/V superlattice (filled black circles)¹³ which is in a weakly tensile strain state. The FeV/V superlattice has a higher expansion in the low concentration region compared to MoV/V but the difference is much smaller in the high concentration region.

IV. DISCUSSION

These results can be discussed in relation to previous measurements of bulk vanadium and superlattices where vanadium is under different strain states. The expansion coefficient of bulk vanadium in the α phase is $k_b=0.191(3)$ and when the expansion is isotropic, the volume change in each of the crystallographic directions can be found by $k_{b,x,y,z}=(1+k_b)^{1/3}-1$. We neglect as a first approximation, the slight asymmetry in the dipole force components. To compare this to the film expansion coefficient k_f we have to account for clamping to the substrate. As stated in Sec. II D, the film expansion is reversible and restricted to the z direction. Using the arguments put forward by Laudahn,³³ we account for the clamping using the generalized expression of the elastic response (Hooke's law),

$$\epsilon_{ij} = \frac{1+\nu}{E} \sigma_{ij} - \delta_{ij} \frac{\nu}{E} \sum_k \sigma_{kk}, \quad (10)$$

where ϵ_{ij} is the strain, ν is Poisson's ratio, E is Young's modulus, δ_{ij} is the Kronecker delta function, and σ_{ij} is the stress tensor. The influence of clamping can be obtained by the following scheme: first we consider isotropic expansion in all crystallographic directions. The influence of biaxial clamping is thus obtained by compressing the in-plane lattice (x, y) to its original value $(-k_{b,z})$. The clamping induced expansion in the z direction is thereby obtained from the resulting elastic response in the z direction. The stresses are unknown but due to symmetry the x and y components are equal and the z component of the strain can be written as

$$\epsilon_{zz} = -\frac{2\nu}{E} \sigma_{xx}. \quad (11)$$

The stress is related to the compressive strain by

$$\sigma_{xx} = -k_{b,z} \frac{E}{1-\nu}. \quad (12)$$

Combining Eqs. (11) and (12) and adding the initial strain due to hydrogen in the z direction, one obtains

$$k_f = k_{b,z} \left(1 + \frac{2\nu}{1-\nu} \right). \quad (13)$$

Using the bulk value³⁴ for Poisson's ratio $\nu=0.342(2)$, we get $k_f=0.122(6)$, which should be compared to the measured slopes [0.21(2) and 0.228(8)]. This result hinges on (i) applicability of the bulk value of ν to the superlattice structure and (ii) negligible influence of deuterium or temperature on ν . We find that the expansion coefficients are larger than would be expected from a triaxial strain field, obtained by occupation of tetrahedral sites.

It is known from bulk VD_x that deuterium occupies the octahedral z (O_z) sites in the β phase. In Fe/V superlattices, loaded with hydrogen it has been shown that hydrogen prefers to occupy the same types of sites (O_z) at all concentrations and temperatures. Thus it seems natural to compare the expansion coefficient with an exclusive O_z site occupancy and include the effects of clamping.

To estimate the expansion coefficient in the z direction with octahedral site occupancy, we consider the following hypothetical situation. Let us assume that deuterium occupies octahedral z sites in the same atomic arrangement as in the bulk β phase. The deuterium-free lattice of bulk vanadium has a body-centered-cubic lattice with $a=0.303$ nm and the β configuration is body centered tetragonal with $a=b=0.3011$ nm and $c=0.3295$ nm for $\text{VD}_{0.5}$.³⁵ We proceed as in the previous example by allowing the film to expand freely in the out of plane direction (and contract in the plane) followed by an expansion in the plane to account for the clamping and consequently a slight contraction out of plane. Since the lattice parameters in the β configuration are at a specific concentration (0.5 D/V) we can extrapolate an expansion coefficient by dividing by the concentration as follows:

$$k_{\text{f}}^{\beta} = \frac{1}{0.5} \frac{\Delta c}{a_0} - \frac{1}{0.5} \frac{2\nu}{1-\nu} \frac{\Delta a}{a_0} \approx 0.16. \quad (14)$$

This is the expected expansion coefficient assuming an exclusive octahedral z site occupancy at all concentrations and is lower than the experimentally determined coefficients. The measured coefficients thus cannot be explained by only taking clamping into account. The results force us to draw the conclusion that by clamping the system in a biaxial compressive strain state, the one-dimensional expansion is larger than the three-dimensional volume expansion in the bulk.

Andersson *et al.* found a nonlinear hydrogen-induced expansion of a symmetric Fe/V superlattice¹⁸ as shown in Fig. 6. Due to the thicker iron layers used in that study, the initial strain state of the superlattice is much higher than considered here. At interior concentrations below 0.1 the expansion was 0.35(1) but at higher concentrations approached the bulk value. However, the accuracy of the measurements hinders quantitative analysis in the low concentration region. Thus, we cannot rule out the large expansion coefficient for deuterium as previously observed for hydrogen at concentrations below 0.1 by Andersson *et al.*¹⁸

There seem to be at least two possible reasons for the difference between our results and those obtained by Andersson *et al.*¹⁸ First, the methodology employed by Andersson *et al.* for determining the volume changes was based on x-ray diffraction, which has recently been called into question.¹⁹ An overestimation of around 20% at intermediate concentrations between the actual volume change and that measured by x-ray diffraction were found in Fe/V 1/7 superlattices. If the overestimation is the same this would explain the bulk of the discrepancy. Second, there could be an isotope dependence on the expansion coefficient in these structures. No isotope effects are observed in the volume expansion in bulk vanadium, when the isotopes are occupying same sites. Thus, different specific volumes of the isotopes appear to be unlikely in the current context.

A concentration dependence of the expansion coefficient was obtained from vanadium under an initial biaxial tensile strain state (MoV/V).¹³ The expansion coefficient was found to change with concentration at 0.2 D/V, measured at 400 K. A change from tetrahedral to octahedral occupancy at concentrations around 0.2 D/V was inferred to cause the change in expansion. The root of the change in occupancy is the opening of the octahedral z sites with increasing tetragonal distortion of the vanadium layers. For the FeV/V superlattice, the initial tetragonal distortion without deuterium is already larger than would be required based on the MoV/V data which would lead us to expect O_z occupancy already at low concentrations.

We suggest the following model to understand these effects. First, since the loading procedure is reversible the transition must be coherent. If the transition is coherent the phases must be similar with respect to crystal symmetry and specific volume. If both phases have O_z site occupancy the transition is much more similar to the β - β_2 phase in bulk vanadium hydride. Interestingly no β_2 phase is observed in VD_x. However the β_2 phase is recovered when external applied stress is applied to the system which suggests that this

situation is plausible.³⁶⁻³⁹ What we could be observing is a density driven transition. At low concentration the elastic dipoles are far apart and contribute to the expansion linearly. In the transition region, the deuterium atoms are closer together and some of the elastic field can be cancelled out, yielding a lower expansion than at low concentrations. At concentrations beyond the end of the plateau the deuterium atoms are closer still but could be much more ordered resulting in no cancellation of the fields. The expansion is even larger than the bulk volume expansion which leads us to conclude that when the initial strain state is biaxial compressive and the volume expansion is forced to be one-dimensional, a spectacular cooperative interplay between the elastic fields takes place.

V. CONCLUSIONS

Isotherms obtained by direct concentration measurements show a well-defined plateau, hinting at the presence of a coexistence region, similar to what is found in bulk. The coexistence however must be made up of phases which are coherent in contrast to bulk since the loading procedure is completely reversible. This is in stark contrast to previous studies on the effect of hydrogen in vanadium-based superlattices where no well defined coexistence region has been reported. The elastic response from the (001) oriented Fe_{0.5}V_{0.5}/V (6/21 ML) superlattice is found to be concentration dependent and a kink is observed at 0.1 and 0.35, which correlates with the plateau. The expansion coefficient is determined to be $k=0.228(8)$ at concentrations below 0.1 and 0.21(2) at concentrations above 0.35. By applying continuum linear elasticity theory one can account for clamping and the expansion coefficient is found to be larger than would be expected for both tetrahedral and octahedral occupancy.

No temperature dependence is found, consistent with bulk results. A model that explains these observations consists of a density-driven disorder/order transition where deuterium occupies the same type of site (probably O_z sites). In the coexistence region the elastic fields could be such that they cancel some of the expansion due to near-field effects, resulting in a lower expansion. At high concentrations, a larger expansion is found which could be due to the ordering of deuterium and no cancellation can take place. These results illustrate the tremendous impact of one-dimensional confinement. By clamping, no in-plane expansion is allowed and the very nature of the phase transition changes from being incoherent to coherent.

ACKNOWLEDGMENTS

We are grateful to Charles Majkrzak and Terrence Udovic at NIST, for valuable discussions and assistance during the neutron experiments. We are indebted to Klaus Leifer and John Timo Wätjen of Uppsala, Department of Engineering Sciences for the guidance and assistance with the TEM analysis. The Swedish research council (VR) and Knut and Alice Wallenberg (KAW) are acknowledged for financial support.

- ¹B. Hjörvarsson, J. A. Dura, P. Isberg, T. Watanabe, T. J. Udovic, G. Andersson, and C. F. Majkrzak, *Phys. Rev. Lett.* **79**, 901 (1997).
- ²F. Klose, C. Rehm, D. Nagengast, H. Maletta, and A. Weidinger, *Phys. Rev. Lett.* **78**, 1150 (1997).
- ³A. Miniotas, R. Brucas, and B. Hjörvarsson, *J. Phys.: Condens. Matter* **13**, L855 (2001).
- ⁴K. C. Kim, B. Dai, J. K. Johnson, and D. S. Sholl, *Nanotechnology* **20**, 204001 (2009).
- ⁵M. Fichtner, *Nanotechnology* **20**, 204009 (2009).
- ⁶M. U. Niemann, S. S. Srinivasan, A. R. Phani, A. Kumar, D. Y. Goswami, and E. K. Stefanakos, *J. Nanomater.* **2008**, 950967 (2008).
- ⁷S. S. Mao and X. Chen, *Int. J. Energy Res.* **31**, 619 (2007).
- ⁸M. Fichtner, *Adv. Eng. Mater.* **7**, 443 (2005).
- ⁹A. Pundt, *Adv. Eng. Mater.* **6**, 11 (2004).
- ¹⁰B. Hjörvarsson, G. Andersson, and E. Karlsson, *J. Alloys Compd.* **253-254**, 51 (1997).
- ¹¹S. Olsson and B. Hjörvarsson, *Phys. Rev. B* **71**, 035414 (2005).
- ¹²G. Reynaldsson, S. Olafsson, and H. Gislason, *J. Alloys Compd.* **356-357**, 545 (2003).
- ¹³V. Leiner, H. Zabel, J. Birch, and B. Hjörvarsson, *Phys. Rev. B* **66**, 235413 (2002).
- ¹⁴G. Andersson, P. Andersson, and B. Hjörvarsson, *J. Phys.: Condens. Matter* **11**, 6669 (1999).
- ¹⁵G. Andersson, B. Hjörvarsson, and P. Isberg, *Phys. Rev. B* **55**, 1774 (1997).
- ¹⁶G. Alefeld and J. Vökl, *Hydrogen in Metals I* (Springer-Verlag, Berlin, 1978).
- ¹⁷F. Stillesjö, B. Hjörvarsson, and H. Zabel, *Phys. Rev. B* **54**, 3079 (1996).
- ¹⁸G. Andersson, B. Hjörvarsson, and H. Zabel, *Phys. Rev. B* **55**, 15905 (1997).
- ¹⁹G. K. Pálsson, A. R. Rennie, and B. Hjörvarsson, *Phys. Rev. B* **78**, 104118 (2008).
- ²⁰Ch. Rehm, H. Maletta, M. Fieber-Erdmann, E. Holub-Krappe, and F. Klose, *Phys. Rev. B* **65**, 113404 (2002).
- ²¹B. Hjörvarsson, M. Vergnat, J. Birch, J.-E. Sundgren, and B. Rodmacq, *Phys. Rev. B* **50**, 11223 (1994).
- ²²V. Sears, *Neutron News* **3**, 26 (1992).
- ²³P. Isberg, B. Hjörvarsson, R. Wäppling, E. Svedberg, and L. Hultman, *Vacuum* **48**, 483 (1997).
- ²⁴M. Björck and G. Andersson, *J. Appl. Crystallogr.* **40**, 1174 (2007).
- ²⁵L. Parratt, *Phys. Rev.* **95**, 359 (1954).
- ²⁶J. A. Dura, D. J. Pierce, C. F. Majkrzak, N. C. Maliszewskyj, D. J. McGillivray, M. Lösche, K. V. O'Donovan, M. Mihailescu, U. Perez-Salas, D. L. Worcester, and S. H. White, *Rev. Sci. Instrum.* **77**, 074301 (2006).
- ²⁷B. Jin and J. Ketterson, *Adv. Phys.* **38**, 189 (1989).
- ²⁸Y. Fukai, *The Metal-Hydrogen System: Basic Bulk Properties* (Springer-Verlag, Berlin, 2005).
- ²⁹A. Remhof, G. Nowak, A. Liebig, H. Zabel, and B. Hjörvarsson, *J. Phys.: Condens. Matter* **18**, L441 (2006).
- ³⁰B. Hjörvarsson, J. Ryden, E. Karlsson, J. Birch, and J.-E. Sundgren, *Phys. Rev. B* **43**, 6440 (1991).
- ³¹B. Hjörvarsson, J. Birch, F. Stillesjö, S. Olafsson, J.-E. Sundgren, and E. Karlsson, *J. Phys.: Condens. Matter* **9**, 73 (1997).
- ³²B. Hjörvarsson, F. Stillesjö, S. Olafsson, E. Karlsson, J. Birch, and J.-E. Sundgren, *J. Magn. Magn. Mater.* **126**, 612 (1993).
- ³³U. Laudahn, S. Fahler, H. Krebs, A. Pundt, M. Bicker, U. Hulsén, U. Geyer, and R. Kirchheim, *Appl. Phys. Lett.* **74**, 647 (1999).
- ³⁴G. Alers, *Phys. Rev.* **119**, 1532 (1960).
- ³⁵H. Asano, L. Abe, and M. Hirabayashi, *Acta Metall.* **24**, 95 (1976).
- ³⁶H. D. Carstanjen, *Z. Phys. Chem.* **165**, 141 (1989).
- ³⁷M. Takakusaki, T. Kajitani, and M. Hirabayashi, *J. Less-Common Met.* **129**, 47 (1987).
- ³⁸Y. Fukai, K. Watanabe, and A. Fukizawa, *J. Less-Common Met.* **88**, 27 (1982).
- ³⁹Y. Fukai, K. Watanabe, and A. Fukizawa, *Phys. Lett. A* **90**, 429 (1982).